The Dietary Charred Meat Carcinogen 2-Amino-1-Methyl-6-Phenylimidazo[4,5-*b*]Pyridine Acts as Both a Tumor Initiator and Promoter in the Rat Ventral Prostate

Yasutomo Nakai,[4] William G. Nelson,[1,2,3] and Angelo M. De Marzo[1,2,3]

Departments of [1]Pathology, [2]The Sidney Kimmel Comprehensive Cancer Center, and the [3]Brady Urological Research Center at Johns Hopkins University School of Medicine, Baltimore, Maryland; and [4]Department of Urology, Osaka University, Osaka, Japan

Abstract

Exposure of Fisher344 rats to 2-amino-1-methyl-6-phenylimidazo[4,5-*b*]pyridine (PhIP), a heterocyclic amine in cooked meat, causes cancer in the rat ventral prostate, while sparing the dorsolateral and anterior lobes. Uncovering the molecular mechanisms of the lobe specificity of PhIP-induced rat prostate cancer may provide clues to the pathogenesis of human prostate cancer, which is also lobe selective. We examined the prostate and other organs for mutation frequencies using transgenic Fisher344 rats (Big Blue rats) after PhIP treatment. After PhIP treatment for as early as 4 weeks, the colon, spleen, seminal vesicles, and all lobes of the prostate had significantly elevated mutation frequencies compared with the saline-treated control group, and the differences became even greater after 8 weeks. G:C → T:A transversions were the predominant type of mutation. After 8 weeks of treatment with PhIP, the Ki-67 index was increased ($P < 0.001$) in the ventral prostate, but not in the dorsolateral or anterior prostate. An increase in the number of stromal mast cells and macrophages was seen in the ventral prostate, but not in the other prostatic lobes. The apoptotic index also increased in the ventral lobe only. The increased proliferation and cell death in response to PhIP indicates that in addition to PhIP acting as an "initiator" of cancer, PhIP is also acting like an organ- and lobe-specific tumor "promoter." The prostate lobe-specific infiltration of mast cells and macrophages in response to PhIP suggests a potential new mechanism by which this dietary compound can increase cancer risk—by prompting inflammation. [Cancer Res 2007;67(3):1378–84]

Introduction

Prostate cancer is the most common noncutaneous malignancy and the second leading cause of cancer-related death in men in the United States. Studies of identical twins have revealed a strong hereditary component to prostate cancer, accounting for ~40% of the overall risk (1). Because roughly 60% is unaccounted for by heredity, however, a significant component of the risk for developing prostate cancer must be related to environmental exposures. What are the environmental exposures that increase prostate cancer risk?

There are two long-standing findings that may provide help in answering this question: (*a*) the incidence and mortality rate of prostate cancer vary worldwide, with the highest rates in the United States and the lowest rates in China and Japan (2); and (*b*) there is an increased risk of prostate cancer in men who immigrated to the United States from China and Japan that begins within one generation after migration (3–5). One major distinction between men from Western cultures and those from East and Southeast Asian cultures is a marked difference in diet. Traditionally, diets rich in vegetables and fruits are consumed in Southeast Asian countries, whereas diets rich in red meat and animal fat, and low in vegetables and fruits, are consumed in Western cultures. Although not unequivocal, there is epidemiologic evidence of a link between prostate cancer incidence and mortality and consumption of red meat and animal fats (6–9).

The biological mechanism by which a diet rich in red meat leads to cancer has not been fully established. Although red meats contain polyunstaturated fatty acids that may accelerate cancer formation by a number of mechanisms (i.e., free-radical formation during oxidative stress, effects on sex hormone levels, direct signaling affecting cell growth and apoptosis; ref. 10), another mechanism may relate to the cooking of meat at high temperatures (e.g., grilling, broiling or frying), which results in the formation of heterocyclic amines (HCA; ref. 11). HCAs can be metabolized to biologically active metabolites that form DNA adducts, which lead to mutations and to organ-specific cancers. 2-Amino-1-methyl-6-phenylimidazo[4,5-*b*]pyridine (PhIP) is the most abundant HCA present in well-done and charred meats (12). Exposure of laboratory rats to PhIP in the diet results in several tumor types, including carcinomas of the intestine in both sexes, in the mammary gland in females, and in the prostate in males (11, 13–15). Cancers in these tissues in humans have all been associated with PhIP exposure to some extent (6, 16–18), and all of these cancers are common in Western countries and infrequent in Southeast Asian countries (19). These same cancers are increasing rapidly in Japan in parallel with the "westernization" of the diet (20).

Exposure of Fisher344 rats to dietary PhIP for 20 weeks results in the development of localized invasive prostatic carcinomas when examined after ~52 weeks (21, 22). The carcinomas are lobe specific in that they develop in the ventral lobe of the prostate but not the dorsolateral or anterior lobes (21). This finding is intriguing because human prostate cancer is also zone specific, in that most cancers arise in the peripheral zone with less arising in the transition zone and almost none arising in the central zone (23). Therefore, uncovering the molecular mechanisms of the lobe specificity of PhIP-induced cancer in the rat prostate may provide clues to the molecular mechanisms for the lobe specificity of cancer in the human prostate.

There are several possible explanations for the lobe selectivity of PhIP-induced cancers in the rat. Cancer induction requires

Requests for reprints: Angelo M. De Marzo, Room 153, Bunting-Blaustein Cancer Research Building, Sidney Kimmel Comprehensive Cancer Center at Johns Hopkins, 1650 Orleans Street, Baltimore, MD 21231-1000. Phone: 410-614-5686; Fax: 410-502-9817; E-mail: ademarz@jhmi.edu.

doi:10.1158/0008-5472.CAN-06-1336

both "initiation" and "promotion." Exposures that initiate cancer are known to induce mutations, whereas those that promote cancer are known to increase the proliferation index. It is not clear whether the ventral lobe of the rat prostate is undergoing selective initiation, promotion, or both in response to PhIP.

In terms of initiation, the accumulation of PhIP-DNA adducts in response to dietary exposure has been examined in the prostate lobes separately, and all lobes similarly form these adducts (21). It is clear, however, that whereas adducts are required for mutations, they may not be sufficient (24). The mutation frequency and spectra in response to PhIP treatment can be monitored using Fisher344 "Big Blue rats," which are transgenic for a phage λ shuttle vector (25). Stuart et al. used this model to show that after as little as 61 days of dietary PhIP exposure, there is an ~20-fold increase in the mutation frequency in the rat prostate (26). Because the entire rat prostate was used in the study by Stuart et al., the lobe specificity of prostate mutations in the rat in response to PhIP has not been previously examined (26). Thus, it is critical to determine whether the ventral lobe is more susceptible to PhIP-induced mutations because this could help to explain the lobe specificity of PhIP-induced prostate cancer.

In terms of tumor promotion, a proliferative index has been assessed in all prostate lobes in response to 4 weeks of PhIP treatment (21). Although Shirai reported a small but significant increase in 5-bromodeoxyuridine uptake in the ventral and dorsolateral lobes in response to PhIP, the lobe specificity of mutations, proliferation rate, and histopathologic changes have not been examined in the same setting in the rat.

Another potential explanation for the lobe selectivity of PhIP-induced prostate cancer may relate to inflammation because several animal models of cancer have been shown to require an inflammatory response for the cancers to occur (27, 28), and the ventral prostate is known to develop spontaneous chronic inflammation in Fisher344 rats that is associated with aging. The mechanisms by which inflammation can increase cancer risk are diverse and may involve initiation, promotion, or both (27). It is important, therefore, to determine whether inflammatory cell infiltrates differ in the different prostate lobes in response to PhIP.

In the present study, we addressed further the molecular mechanisms for the lobe specificity of prostate cancer in the Fisher344 rat by studying the mutation frequency and spectra in each lobe (separately isolated) of the prostate after short-term PhIP treatment. We also compared the mutation frequency and spectra to those found in other organs that are targets of PhIP-induced carcinogenesis (colon and spleen) and those that are not (liver, kidney, and seminal vesicles). In addition, we examined histopathologic and immunophenotypic changes in response to PhIP exposure in each prostate lobe, including cell proliferation rate, and inflammatory cell infiltrates.

Materials and Methods

Chemicals. PhIP hydrochloride was obtained from the NARD Institute (Osaka, Japan) with purity above 99.9%.

Animals and treatment. Male Big Blue transgenic Fisher344 rats (13–15 weeks old) were purchased from Stratagene (La Jolla, CA). Rats were housed in an animal facility maintained on a 12-h light-dark cycle, at a constant temperature (22 ± 2°C) and relative humidity (55 ± 15%). Tap water and food were available *ad libitum*. PhIP was suspended in saline (14 mg/mL) and was given to the rats intragastrically by gavage at the dose of 70 mg/kg (5 mL/kg) thrice a week for 4 weeks (n = 3) and 8 weeks (n = 3). For the control group, 5 mL/kg of saline was given intragastrically thrice a week for 4 weeks (n = 3) and 8 weeks (n = 3). The animal weights were recorded once per week until the end of the experiment. Rats were euthanized by CO_2 asphyxiation at day 30 for the 4-week treatment group and at day 60 for the 8-week treatment group. All prostate lobes were dissected separately into anterior, dorsolateral complex, and ventral lobes. In addition, the seminal vesicles, liver, kidney, spleen, and colon were immediately dissected. Half of each tissue was flash-frozen in liquid nitrogen and then stored at −80°C. The rest of the tissues were fixed in 10% buffered formalin and examined by routine light microscopy.

Isolation of DNA. DNA was isolated using the RecoverEase protocol (Stratagene). Briefly, 40 to 60 mg of tissue from the different prostate lobes (anterior, ventral, and dorsolateral), seminal vesicles, liver, kidney, spleen, and liver were disaggregated using a Wheaton Dounce tissue grinder, and cell nuclei were collected by centrifuge at 1,100 × g for 12 min. Nuclear pellets were treated with proteinase K and RNAce-It (Stratagene) for 45 min at 50°C and were dialyzed against 10 mmol/L Tris/1 mmol/L EDTA buffer (pH 7.5) for 48 h. The viscous DNA was stored at 4°C until packaging.

Lambda *cII* mutation analysis. Big Blue rats contain a λLIZ shuttle vector that includes the *cII* gene, which is the target for the mutagenesis studies. The *cII* gene plays a critical role in the decision between lysis or lysogeny of λ phage following infection of *Escherichia coli*. In *hfl*$^-$ bacteria, the cII protein is not degraded, and it activates transcription of the *cI* repressor. The cI protein, in turn, inhibits the transcription of several genes essential for the lytic response. This results in continuous lysogeny and with no plaque formation. When there is an inactivating mutation in the *cII* gene, the *cI* gene is not transcribed, and plaques arise, which enables the number of mutant plaques under selective conditions (24°C) to be determined. Because the λLIZ shuttle vector contains the temperature-sensitive *cI*857 mutation, which inactivates the cI repressor at 37°C, the phage multiplies through the lytic cycle under nonselective conditions (37°C), resulting in plaque formation regardless of the status of the *cII* gene. This allows the calculation of the number of recovered phage genomes or the phage titer. The mutation frequency is calculated by dividing the number of mutant plaques by the phage titer.

We used the λ *Select-cII* mutation detection system for Big Blue rodents (Stratagene) for the lambda *cII* assay. The kit contains the Transpack packaging extract and *hfl*$^-$ *E. coli* G1250. Genomic DNA (8 μL) was incubated in the red tube of the Transpack packaging extract for 90 min at 30°C, and then 12 μL of the Transpack packaging extract from the blue tube was transferred to the red tube and incubated for 90 min at 30°C. Following the incubation, 1.1 mL of SM buffer [100 mmol/L NaCl, 8 mmol/L $MgSO_4 \cdot 7H_2O$, 50 mmol/L Tris-HCl (pH 7.5), 0.01% gelatin] was added to each packaging reaction. One hundred microliters of packaged λ phage solution was mixed with 200 μL of G1250 at room temperature for 30 min, mixed with 2.5 mL TB1 top agar, and plated on ten 10-cm dishes containing 25 mL bottom agar. The plates were incubated at 24°C for 48 h. For titration, a 100-μL aliquot of a 1:100 dilution of the packaged λ phage solution was mixed with 200 μL of G1250 and 2.5 mL TB1 top agar, plated on three dishes, and incubated at 37°C for 24 h.

Sequencing of *cII* mutants. To validate whether presumptive mutant plaques actually represented phage genomes containing a mutant *cII* gene, plaques obtained at 24°C were analyzed for *cII* gene sequence mutations. When the number of mutant plaques exceeded 40 per assay, 10% to 30% of mutant plaques were sequenced for the *cII* gene. The *cII* gene was amplified by PCR using primer pair 5′-CCGCTCTTACACATTCCAGC-3′ and 5′-CCTCTGCCGAAGTTGAGTAT-3′. The amplified *cII* gene length is 294 bp, and the total PCR fragment is 476 bp. The amplified *cII* gene was purified by the Rapid 96 PCR Purification System (Marligen Bioscience, Ijamsville, MD). DNA sequencing was done using an ABI Prism 3730 Genetic Analyzer (Applied Biosystems, Foster City, CA), and the sequence was analyzed using Sequencher v4.1.4 (Gene Codes Corporation, Ann Arbor, MI).

Antibodies. Anti–Ki-67 antibody (rabbit polyclonal, dilution 1:4,000) was from Novocastra (Newcastle-upon-Tyne, United Kingdom). Antirat CD68

antibody (mouse monoclonal, clone ED1, dilution 1:2,000) was from Serotec (Oxford, United Kingdom). Anti-glutathione-*S*-transferase antibody (rabbit polyclonal, dilution 1:1,250) was from Lab Vision (Fremont, CA). Anticleaved caspase 3 antibody (rabbit polyclonal) was from Cell Signaling Technology (Beverly, MA).

Histology and immunohistochemistry. Histologic examination was done on paraffin-embedded sections after H&E staining. Immunohistochemistry was done using the EnVision+ detection system (DAKO, Carpinetria, CA). Briefly, paraffin sections were deparaffinized and rehydrated through a graded alcohol series. For Ki-67 and GSTP1 staining, steam heating in Target Retrieval Solution (DAKO) for 40 min was done. For cleaved caspase 3 and CD68 staining, steam heating in Antigen Unmasking Solution (Vector Laboratories, Burligame CA) for 20 min was done. Primary antibodies were incubated for 45 min at room temperature (Ki-67, CD68, cleaved caspase 3) or overnight at 4°C (GSTP1). Slides were counterstained with hematoxylin.

Assessment of immunostaining. Ki-67 and caspase 3 staining was evaluated by quantitative analysis using the Chromavision ACIS (Clarient, San Juan Capistrano, CA). At least 10 regions were randomly chosen from each rat, and prostatic epithelial cells were circled on the computer monitor, and brown area (positive staining) and blue area (nuclei not immunostained) in the regions were counted. The Ki-67 labeling index and apoptosis index were obtained by dividing the brown area by the brown area plus the blue area.

Mast cell staining. Paraffin-embedded sections were deparaffinized with xylene and stained with 0.1% toluidine blue in 1% sodium chloride solution. Staining with toluidine blue permits the identification of mast cells because mast cell granules stain metachromatically, resulting in deep purplish-blue granular cytoplasmic staining.

Mast cell and macrophage counting. The number of mast cells and macrophages were counted at a magnification of 100× and 200×, respectively, under light microscopy. At least five regions were selected at random for counting, and the average number in each group was determined.

Statistics. The difference of the number of Ki-67–positive cells, caspase 3–positive cells, mast cell number, and macrophage number was analyzed by two-sided unpaired Student's *t* test and considered statistically different when *P* value was <0.05. The correlation between mutation frequencies and mast cell number and the correlation between mast cell number and Ki-67 index were analyzed by linear regression.

Results

Mutation frequencies. The mutation frequencies of the saline-treated rats (negative controls) represent the spontaneous frequencies in each tissue. The spontaneous mutation frequencies in the control rats were not different between the tissues analyzed both after 4 weeks (F = 1.86; P = 0.14) or after 8 weeks (F = 1.36; P = 0.30; one-way factorial ANOVA; Fig. 1). By contrast, after PhIP exposure for either 4 or 8 weeks, the mutation frequencies of the colon, spleen, seminal vesicles, and each lobe of the prostate were significantly greater than their corresponding tissues in the control group (Fig. 1). The liver and kidneys, which do not develop cancer in response to PhIP (11), did not show an increase in their mutation frequencies after exposure to PhIP (Fig. 1).

Mutation spectra. The mutation spectra of the target tissues after 4 and 8 weeks of PhIP treatment are shown in Fig. 2. G:C → A:T transitions, G:C → T:A, G:C → C:G transversions, and single base-pair deletions were significantly increased.

The most frequently deleted base was guanine (data not shown). Overall, these types of mutations are similar to that expected after PhIP treatment (29–31).

Histology and histochemistry. By standard H&E staining, there were no differences in morphology within the epithelial compartment between the various prostate lobes of the PhIP-treated and untreated animals after either 4 or 8 weeks of exposure to PhIP. However, when analyzed for epithelial cell proliferation in response to PhIP treatment by immunostaining for Ki-67, the dorsolateral and anterior lobes showed virtually no change, yet the ventral prostate showed a marked increase in staining (Fig. 3*A–F*). This increase in the proliferative fraction of epithelial cells was statistically significant both after 4 and 8 weeks of PhIP exposure (Fig. 3*G*; 4-week data is not shown). In terms of cell death, very few apoptotic cells were seen in the ventral prostate of the saline-treated rats after 8 weeks, but when treated with PhIP, there was an increase in apoptosis (from 0% to ~0.1%) as detected by immunostaining for activated caspase 3 (data not shown).

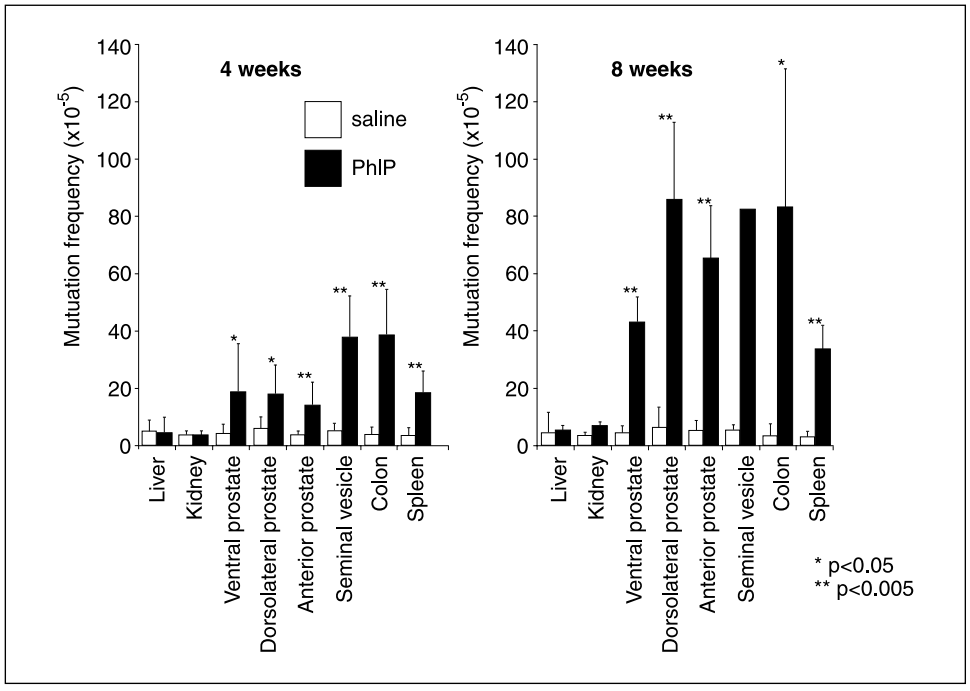

Figure 1. Mutation frequencies after 4 wks (*left*) and 8 wks (*right*) of PhIP treatment. Each tissue and prostate lobe was collected and subjected to λ *cII* mutation analysis. *Columns,* means (n = 3); *bars,* SE. Student's *t* test analysis: *, P < 0.05; **, $P \leqslant 0.005$ compared with the saline group and PhIP group in each tissue.

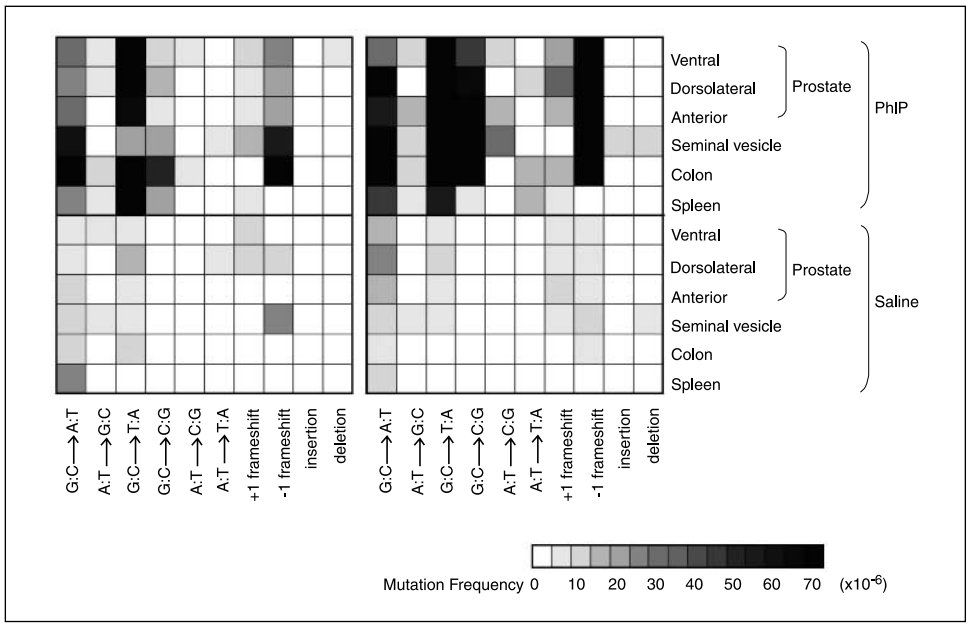

Figure 2. Mutation frequency and spectra in the *cII* gene after 4 wks (*left*) and 8 wks (*right*) of PhIP treatment. In the control animals, G:C to A:T transition mutation was the most frequently seen mutation. After PhIP treatment, G:C to T:A transversions, followed by −1-bp deletions (most of them were guanine deletion) were the most frequently seen types of mutation.

In the stromal compartment of the ventral prostate, standard H&E staining revealed an increase in mononuclear cells in which blue granules were seen in the cytoplasm. These cells were confirmed to be mast cells by staining with toluidine blue (Fig. 4*A* and *B*). After both 4 and 8 weeks of PhIP treatment, the number of mast cells was significantly increased only in the ventral prostate (Fig. 4*E*), and this increase correlated with the mutation frequencies (r = 0.867; P = 0.0003). Although there was no spatial relation between individual mast cells and proliferating epithelial cells, as determined by Ki-67 staining with toluidine blue counterstaining (data not shown), there was a strong correlation between the number of mast cells and the proliferation index (r = 0.937; P < 0.0001). The number of macrophages, which were labeled by CD68 staining, was also increased in the ventral prostate only both after 4 and 8 weeks of treatment with PhIP (Fig. 4*C* and *D*). The number of macrophages also correlated with the proliferation index (r = 0.629; P = 0.029).

Because the π class glutathione *S*-transferase gene (*GSTP1*) is inactivated in human prostate cancer by the promoter region CpG island hypermethylation and can prevent PhIP-induced DNA adduct formation in human prostate cancer cells in culture (32, 33), we also examined the pattern of GSPT1 protein expression in the

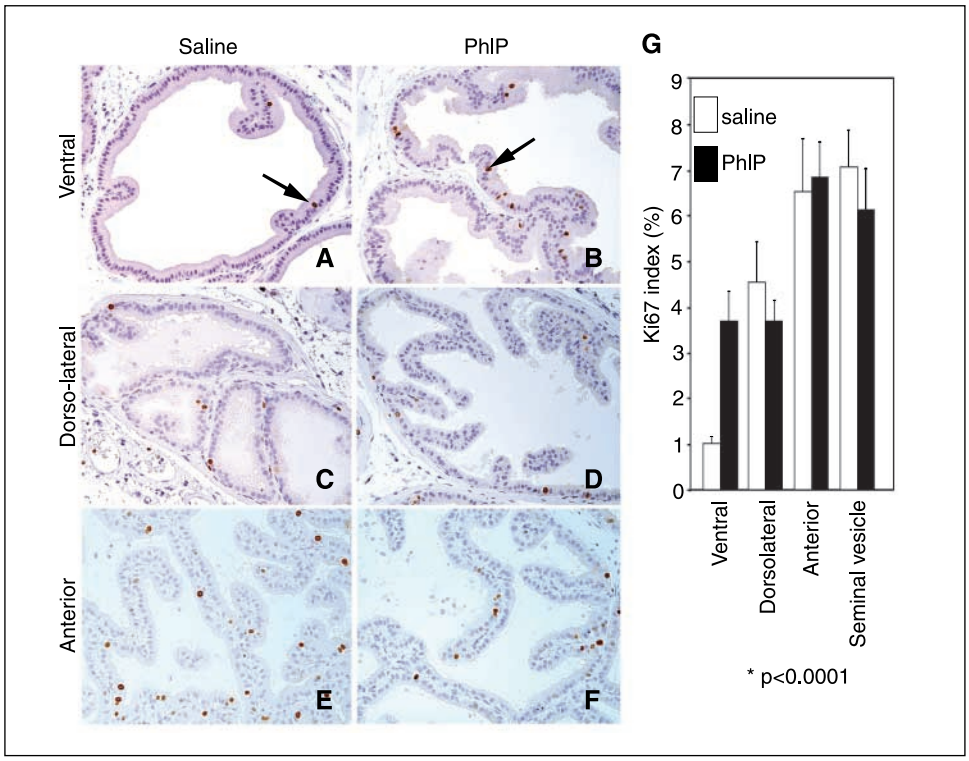

Figure 3. Ki-67 staining (*A–F*) of the prostate after 8 wks of saline (*left*) and PhIP (*right*) treatment. *G,* the ratio of the positive cells was analyzed by the Chromavision ACIS II (Clarient, San Juan Capistrano, CA). *Columns,* means of the positive cell ratio (%) of the 30 areas from each group; *bars,* SE. Student's *t* test analysis: *, P < 0.0001.

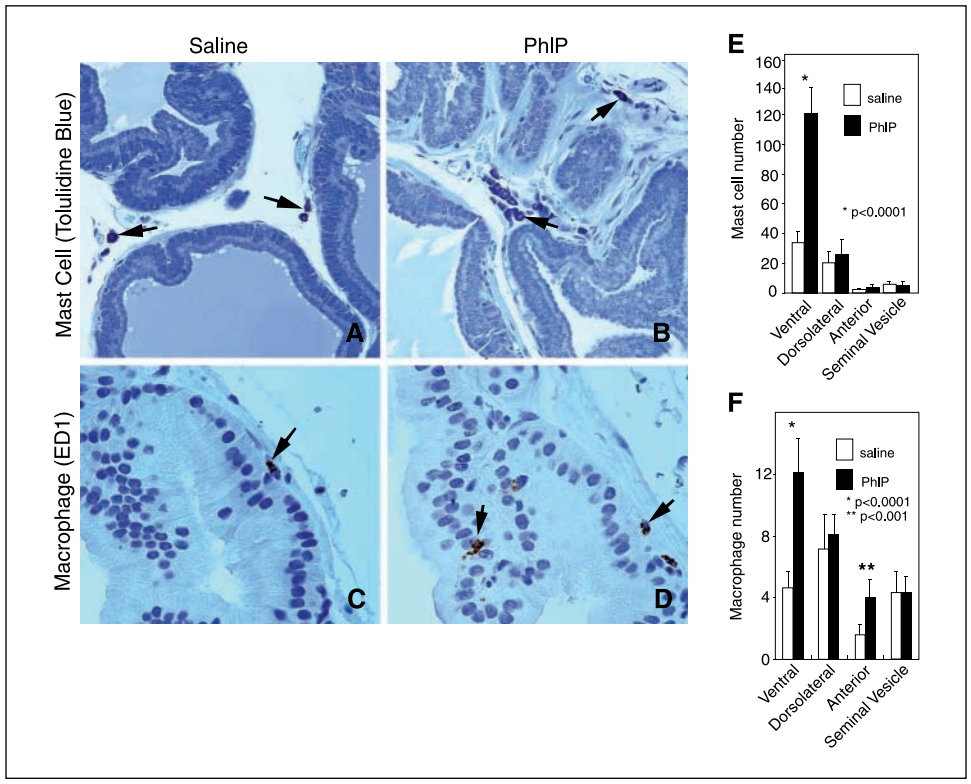

Figure 4. Mast cell (toluidine blue) staining (*A* and *B*) and macrophage (CD68) staining (*C* and *D*) of the ventral prostate. *A* and *C,* saline-treated and (*B* and *D*) PhIP-treated rats (data shown is from the 8-wk treatment groups). *E,* mast cell numbers were counted under microscope at ×100. *F,* macrophage numbers were counted under the microscope at ×200. *Columns,* means of mast cell or macrophage number of the field analyzed in each group; *bars,* SE. *P* values are from the Student's *t* test analysis. *A* and *B, arrows,* mast cells; *C* and *D, arrows,* macrophages.

various lobes of the rat prostate in response to PhIP. Strong GSPT1 staining was seen in basal cells in all lobes, and variable and weaker staining was noted in the luminal cells. However, no change in the extent or pattern of GSTP1 staining was noted after PhIP treatment at either time point.

Discussion

HCAs, of which there are at least 10 chemical forms, are produced from amino acids, creatine/creatinine, and polysaccharide precursors during the high-temperature cooking of meats and fish (12). PhIP, which is the most abundant of the HCAs found in cooked meats, has been shown to be carcinogenic in the prostate, mammary gland, intestine, and lymphoid tissue in experimental animal studies (34–36). The major pathway of HCA activation involves phase I hepatic cytochrome P450–mediated N-hydroxylation followed by phase II esterification of the *N*-hydroxylamines to reactive ester derivatives. These derivatives spontaneously degrade to arylnitrenium ions and form DNA adducts by covalent binding, mainly to the C8 position of guanine. If not repaired, these DNA adducts can result in base substitution mutations, small deletions, and small insertions (37). Cui et al. showed that in human prostate xenografts, PhIP-DNA adducts can be detected after exposing mice to PhIP intragastically (38), and Nelson et al. showed that in human explants of prostate tissues, *N*-hydroxy PhIP can be metabolized to adduct-forming derivatives (32). These studies indicate that the human prostate can be a target of dietary PhIP-induced adducts.

In this study, we found that the colon, spleen, seminal vesicles, and all lobes of prostate are target tissues of PhIP-induced mutations. In these tissues, 4 weeks was sufficient to induce mutations. The type of mutations most frequently observed were G:C to A:T transitions followed by G:C to T:A transversions, G:C to C:G transversions, and −1-bp deletions in these target tissues. These types of mutations were similar to that expected after PhIP treatment (29), suggesting that these mutations were caused by PhIP-DNA adducts.

The tissue specificity of PhIP-induced mutations in this study (liver and kidney did not show increases, and the prostate, seminal vesicles, and colon did show increases) suggests that PhIP-induced mutations require cell proliferation—liver and kidney epithelial cells turn over extremely slowly, whereas splenocytes, colonic epithelial cells, prostate epithelial cells, and seminal vesicle epithelial cells have a variable yet much higher turnover rate than the liver or kidney. However, not all of these target tissues of PhIP-induced mutations are the target tissues of PhIP-induced cancer (11). Despite the present study's finding that all prostate lobes and seminal vesicles were target tissues for mutation, only the ventral lobe is known to develop prostate cancer in this rat model. Nagao et al. reviewed the association between DNA adducts, mutation, and cancer incidence and did not find a strong correlation between mutation frequency and cancer incidence (24). This fact suggests that whereas mutations, which are related to the initiation of cancer, are required for malignant transformation, there must be other factors, such as tumor "promoters," required for the cancer occurrence in response to PhIP.

To further examine the link between PhIP-induced mutations and prostate lobe–specific carcinogenesis, we analyzed the prostate lobe–specific phenotypic responses to PhIP. In the dorsolateral prostate, anterior prostate, and seminal vesicle, there was no change in proliferation in response to PhIP. However, in the ventral prostate, there was a significant increase in proliferation after exposure to PhIP. An increase in proliferation in response to PhIP has also been reported in other target tissues. In a PhIP-induced rat mammary cancer model, proliferation of the epithelial cells of the mammary gland terminal end buds, putative sites of origin of carcinomas, increased after exposure to PhIP (39), and Shirai has previously reported an increase in proliferation in all

prostate lobes in response to PhIP (21). It is unclear why we found in the present study an increase in proliferation only in the ventral lobe. Nevertheless, these findings suggest that PhIP is acting as both an initiator and promoter of cancer in the ventral prostate. What might be responsible for this increased proliferation?

One potential mechanism may relate to the finding that PhIP has an estrogenic effect and can stimulate cell proliferation through estrogen receptor α (31, 40). Fujimoto et al. showed that estrogen receptor α mRNA is expressed in the rat ventral prostate (41), and that estrogen and testosterone together up-regulated the expression of estrogen receptor α mRNA (41). In addition, estrogen, along with testosterone, resulted in increased expression of androgen-responsive genes (41). Estrogens can induce prostate inflammation in the rat and have been postulated to play a role in increasing the risk for human prostate cancer (42). Whether estrogen receptor signaling is involved in PhIP-induced prostate carcinogenesis awaits further study.

Another potential novel mechanism by which PhIP may indirectly influence prostate carcinogenesis in the ventral prostate may relate to our finding that mast cells and macrophages accumulated selectively in the ventral prostate in response to PhIP treatment. Recent experiments indicate that mast cell infiltration can enhance carcinogenesis (43, 44). Mast cells contribute to the development of skin cancer in K14-HPV16 transgenic mouse by releasing proteases, such as tryptase and chymase, and stimulating angiogenesis (45). In a 1,2-dimethylhydrazine–induced intestinal tumor model, the incidence of intestinal cancer was significantly reduced in mast cell–deficient $Kit^{W}/Kit^{W\text{-}v}$ mice, whereas when the mast cells were rescued by bone marrow transplantation, the cancer incidence was the same as the normal mice treated with 1,2-dimethylhydrazine (46). Although the mechanisms by which mast cells contribute to carcinogenesis are not understood, mast cells play an important role in the initiation of inflammation. Mast cells are the only tissue-resident cells with granules containing preformed tumor necrosis factor α, and releasing this cytokine from mast cells is important for the initiation of an inflammatory response (47). In this study, along with mast cell infiltration in the ventral prostate, the number of macrophages was increased in the ventral prostate after PhIP treatment. This increase of macrophages might partly be due to the cytokines released from infiltrating mast cells. Macrophages have been shown clearly to aid in both the initiation and progression of experimental cancers (48–50). Although our study was conducted for 8 weeks, we have now done additional longer term studies in the same model system. In our preliminary analysis, we have reproduced the findings of Shirai et al. in that the addition of PhIP at 400 ppm to the diet for 20 weeks results in the appearance of intraductal carcinoma lesions at 52 weeks. In this model/paradigm, we have now found similar increases in mast cells, even at 52 weeks, in the PhIP-treated animals. Additional work is needed to determine whether mast cells and/or macrophages are contributing to prostate carcinogenesis in response to PhIP.

In summary, in attempts to begin to elucidate the lobe-specific carcinogenetic effects of the dietary carcinogen PhIP on the rat prostate, we have shown that all prostate lobes accumulate mutations in response to short-term PhIP treatment. Thus, mutations alone, while necessary for cancer formation, do not correlate with subsequent cancer formation. We report for the first time that the ventral prostate selectively responded to PhIP treatment by an increase in stromal mast cells, macrophages, and epithelial cell proliferation. These results suggest that the inflammatory response may help explain the tissue-specific and prostate lobe–specific carcinogenesis in the rat prostate induced by a dietary carcinogen.

Note Added in Proof

After the submission of this manuscript, Borowsky et al. (Neoplasia 2006;8:708–15) reported that PhIP induces acute and chronic inflammation in the prostate prior to inducing PIN and intraductal cancers. Although masts cells and macrophages were not evaluated, and the lobe specificity was not commented upon, these results are consistent with the concept that PhIP may act in part by inducing inflammation in the prostate.

Acknowledgments

Received 4/12/2006; revised 10/2/2006; accepted 12/4/2006.

Grant support: Department of Defense Congressional Dir. Med. Research Program PC050457. Public Health Services NIH/National Cancer Institute R01CA084997, NIH R01CA70196, and NIH/National Cancer Institute Specialized Programs of Research Excellence in Prostate Cancer P50CA58236 (Johns Hopkins) and philanthropic support from the Donald and Susan Sturm Foundation, Bernard L. Schwartz, and Richard Allan Barry. A.M. De Marzo is a Helen and Peter Bing Scholar through The Patrick C. Walsh Prostate Cancer Research Fund.

The costs of publication of this article were defrayed in part by the payment of page charges. This article must therefore be hereby marked *advertisement* in accordance with 18 U.S.C. Section 1734 solely to indicate this fact.

References

1. Isaacs WB, Xu J, Walsh PC. Hereditary prostate cancer. In: Chung LW, Isaacs WB, Simons JW, editors. Prostate cancer: biology, genetics, and the new theraputics. Totowa (NJ): Humana Press; 2001. p. 13–37.
2. Gronberg H. Prostate cancer epidemiology. Lancet 2003;361:859–64.
3. Locke FB, King H. Cancer mortality risk among Japanese in the United States. J Natl Cancer Inst 1980; 65:1149–56.
4. Shimizu H, Ross RK, Bernstein L, et al. Cancers of the prostate and breast among Japanese and white immigrants in Los Angeles County. Br J Cancer 1991;63:963–6.
5. Cook LS, Goldoft M, Schwartz SM, Weiss NS. Incidence of adenocarcinoma of the prostate in Asian immigrants to the United States and their descendants. J Urol 1999;161:152–5.
6. Norrish AE, Ferguson LR, Knize MG, et al. Heterocyclic amine content of cooked meat and risk of prostate cancer. J Natl Cancer Inst 1999;91:2038–44.
7. Carroll PR, Grossfeld GD. American Cancer Society. Prostate cancer, p. xiii, 402 p. Hamilton Lewiston, NY: BC Decker; Sales and Distribution, US, BC Decker, 2002.
8. Giovannucci E, Rimm EB, Colditz GA, et al. A prospective study of dietary fat and risk of prostate cancer. J Natl Cancer Inst 1993;85:1571–9.
9. Michaud DS, Augustsson K, Rimm EB, et al. A prospective study on intake of animal products and risk of prostate cancer. Cancer Causes Control 2001;12:557–67.
10. Kolonel LN, Nomura AM, Cooney RV. Dietary fat and prostate cancer: current status. J Natl Cancer Inst 1999; 91:414–28.
11. Sugimura T, Wakabayashi K, Nakagama H, Nagao M. Heterocyclic amines: Mutagens/carcinogens produced during cooking of meat and fish. Cancer Sci 2004;95: 290–9.
12. Knize MG, Felton JS. Formation and human risk of carcinogenic heterocyclic amines formed from natural precursors in meat. Nutr Rev 2005;63:158–65.
13. Ito N, Hasegawa R, Sano M, et al. A new colon and mammary carcinogen in cooked food, 2-amino-1-methyl-6-phenylimidazo[4,5-*b*]pyridine (PhIP). Carcinogenesis 1991;12:1503–6.
14. Hasegawa R, Sano M, Tamano S, et al. Dose-dependence of 2-amino-1-methyl-6-phenylimidazo[4,5-*b*]-pyridine (PhIP) carcinogenicity in rats. Carcinogenesis 1993;14:2553–7.
15. Rao CV, Rivenson A, Zang E, et al. Inhibition of 2-amino-1-methyl-6-phenylimidazo[4,5]pyridine-induced lymphoma formation by oltipraz. Cancer Res 1996;56: 3395–8.
16. Sinha R, Kulldorff M, Chow WH, et al. Dietary intake of heterocyclic amines, meat-derived mutagenic activity, and risk of colorectal adenomas. Cancer Epidemiol Biomarkers Prev 2001;10:559–62.
17. Bogen KT, Keating GA. U S. dietary exposures to heterocyclic amines. J Expo Anal Environ Epidemiol 2001;11:155–68.
18. Cross AJ, Peters U, Kirsh VA, et al. A prospective study of meat and meat mutagens and prostate cancer risk. Cancer Res 2005;65:11779–84.
19. Parkin DM, Bray FI, Devesa SS. Cancer burden in the

year 2000. The global picture. Eur J Cancer 2001;37 Suppl 8:S4–66.
20. Sim HG, Cheng CW. Changing demography of prostate cancer in Asia. Eur J Cancer 2005;41:834–45.
21. Shirai T, Sano M, Tamano S, et al. The prostate: a target for carcinogenicity of 2-amino-1-methyl-6-phenylimidazo[4,5-*b*]pyridine (PhIP) derived from cooked foods. Cancer Res 1997;57:195–8.
22. Shirai T, Cui L, Takahashi S, et al. Carcinogenicity of 2-amino-1-methyl-6-phenylimidazo [4,5-*b*]pyridine (PhIP) in the rat prostate and induction of invasive carcinomas by subsequent treatment with testosterone propionate. Cancer Lett 1999;143:217–21.
23. McNeal JE, Redwine EA, Freiha FS, Stamey TA. Zonal distribution of prostatic adenocarcinoma. Correlation with histologic pattern and direction of spread. Am J Surg Pathol 1988;12:897–906.
24. Nagao M, Ochiai M, Okochi E, et al. LacI transgenic animal study: relationships among DNA-adduct levels, mutant frequencies and cancer incidences. Mutat Res 2001;477:119–24.
25. Jakubczak JL, Merlino G, French JE, et al. Analysis of genetic instability during mammary tumor progression using a novel selection-based assay for *in vivo* mutations in a bacteriophage lambda transgene target. Proc Natl Acad Sci U S A 1996;93:9073–8.
26. Stuart GR, Holcroft J, de Boer JG, Glickman BW. Prostate mutations in rats induced by the suspected human carcinogen 2-amino-1-methyl-6-phenylimidazo[4,5-*b*]pyridine. Cancer Res 2000;60:266–8.
27. Coussens LM, Werb Z. Inflammation and cancer. Nature 2002;420:860–7.
28. Pikarsky E, Porat RM, Stein I, et al. NF-κB functions as a tumour promoter in inflammation-associated cancer. Nature 2004;431:461–6.
29. Morgenthaler PM, Holzhauser D. Analysis of mutations induced by 2-amino-1-methyl-6-phenylimidazo[4,5-*b*]pyridine (PhIP) in human lymphoblastoid cells. Carcinogenesis 1995;16:713–8.
30. Yadollahi-Farsani M, Gooderham NJ, Davies DS, Boobis AR. Mutational spectra of the dietary carcinogen 2-amino-1-methyl-6-phenylimidazo[4,5-*b*]pyridine(PhIP) at the Chinese hamsters hprt locus. Carcinogenesis 1996; 17:617–24.
31. Gooderham NJ, Zhu H, Lauber S, et al. Molecular and genetic toxicology of 2-amino-1-methyl-6-phenylimidazo[4,5-*b*]pyridine (PhIP). Mutat Res 2002;506–7: 91–9.
32. Nelson CP, Kidd LC, Sauvageot J, et al. Protection against 2-hydroxyamino-1-methyl-6-phenylimidazo[4,5-*b*]pyridine cytotoxicity and DNA adduct formation in human prostate by glutathione *S*-transferase P1. Cancer Res 2001;61:103–9.
33. Lin X, Tascilar M, Lee WH, et al. GSTP1 CpG island hypermethylation is responsible for the absence of GSTP1 expression in human prostate cancer cells. Am J Pathol 2001;159:1815–26.
34. Sugimura T. Overview of carcinogenic heterocyclic amines. Mutat Res 1997;376:211–9.
35. Layton DW, Bogen KT, Knize MG, et al. Cancer risk of heterocyclic amines in cooked foods: an analysis and implications for research. Carcinogenesis 1995;16:39–52.
36. Jagerstad M, Skog K. Genotoxicity of heat-processed foods. Mutat Res 2005;574:156–72.
37. Schut HA, Snyderwine EG. DNA adducts of heterocyclic amine food mutagens: implications for mutagenesis and carcinogenesis. Carcinogenesis 1999;20:353–68.
38. Cui L, Takahashi S, Tada M, et al. Immunohistochemical detection of carcinogen-DNA adducts in normal human prostate tissues transplanted into the subcutis of athymic nude mice: results with 2-amino-1-methyl-6-phenylimidazo[4,5-*b*]pyridine (PhIP) and 3,2'-dimethyl-4-aminobiphenyl (DMAB) and relation to cytochrome P450s and *N*-acetyltransferase activity. Jpn J Cancer Res 2000;91:52–8.
39. Snyderwine EG. Mammary gland carcinogenesis by 2-amino-1-methyl-6-phenylimidazo[4,5-*b*]pyridine in rats: possible mechanisms. Cancer Lett 1999;143:211–5.
40. Lauber SN, Ali S, Gooderham NJ. The cooked food derived carcinogen 2-amino-1-methyl-6-phenylimidazo[4,5-*b*] pyridine is a potent oestrogen: a mechanistic basis for its tissue-specific carcinogenicity. Carcinogenesis 2004;25:2509–17.
41. Fujimoto N, Suzuki T, Honda H, Kitamura S. Estrogen enhancement of androgen-responsive gene expression in hormone-induced hyperplasia in the ventral prostate of F344 rats. Cancer Sci 2004;95:711–5.
42. Coffey DS. Similarities of prostate and breast cancer: evolution, diet, and estrogens. Urology 2001;57:31–8.
43. Dimitriadou V, Koutsilieris M. Mast cell-tumor cell interactions: for or against tumour growth and metastasis? Anticancer Res 1997;17:1541–9.
44. Theoharides TC, Conti P. Mast cells: the Jekyll and Hyde of tumor growth. Trends Immunol 2004; 25:235–41.
45. Coussens LM, Raymond WW, Bergers G, et al. Inflammatory mast cells up-regulate angiogenesis during squamous epithelial carcinogenesis. Genes Dev 1999; 13:1382–97.
46. Wedemeyer J, Galli SJ. Decreased susceptibility of mast cell-deficient Kit(W)/Kit(W-v) mice to the development of 1, 2-dimethylhydrazine-induced intestinal tumors. Lab Invest 2005;85:388–96.
47. Galli SJ, Nakae S, Tsai M. Mast cells in the development of adaptive immune responses. Nat Immunol 2005;6:135–42.
48. Tanaka T, Kohno H, Suzuki R, et al. A novel inflammation-related mouse colon carcinogenesis model induced by azoxymethane and dextran sodium sulfate. Cancer Sci 2003;94:965–73.
49. Greten FR, Eckmann L, Greten TF, et al. IKKβ links inflammation and tumorigenesis in a mouse model of colitis-associated cancer. Cell 2004;118:285–96.
50. Lin EY, Nguyen AV, Russell RG, Pollard JW. Colony-stimulating factor 1 promotes progression of mammary tumors to malignancy. J Exp Med 2001;193: 727–40.